Journal of Materials Chemistry B

# Vessel Graft Fabricated by the Onsite Differentiation of Human Mesenchymal Stem Cells Toward Vascular Cells on Vascular Extracellular Matrix Scaffold under Mechanical Stimulations in A Rotary Bioreactor

| | |
|---|---|
| Journal: | *Journal of Materials Chemistry B* |
| Manuscript ID | TB-ART-12-2018-003348.R1 |
| Article Type: | Paper |
| Date Submitted by the Author: | 04-Mar-2019 |
| Complete List of Authors: | Li, Na; University of South Dakota, Department of Biomedical Engineering; BioSNTR<br>Rickel, Alex; University of South Dakota, Department of Biomedical Engineering; BioSNTR<br>Sanyour, Hanna; University of South Dakota, Department of Biomedical Engineering; BioSNTR<br>Hong, Zhongkui; University of South Dakota, Biomedical engineering; BioSNTR |
| | |

# Vessel Graft Fabricated by the On-site Differentiation of Human Mesenchymal Stem Cells Toward Vascular Cells on Vascular Extracellular Matrix Scaffold under Mechanical Stimulations in A Rotary Bioreactor

Na Li[1,2], Alex P. Rickel[1,2], Hanna J. Sanyour[1,2], Zhongkui Hong[1,2]*

[1]Department of Biomedical Engineering, University of South Dakota, 4800 N Career Ave, Suite 221, Sioux Falls, SD, USA

[2]BioSNTR, Sioux Falls, SD, USA

*To whom correspondence should be addressed:

Zhongkui Hong, Ph.D.,

Biomedical Engineering Department,

University of South Dakota,

4800 N Career Ave, Suite 221, Sioux Falls, SD 57107

Fax: (605) 782-3280

Tel: (605) 275-7468

E-mail: Zhongkui.Hong@usd.edu

**Abstract**

Although a significant number of studies on vascular tissue engineering have been reported, current availability of vessel substitutes in clinic remains limited mainly due to the mismatch of their mechanical properties and biological functions with native vessels. In this study, a novel approach to fabricating a vessel graft for vascular tissue engineering was developed by promoting the differentiation of human bone marrow mesenchymal stem cells (MSCs) into endothelial cells (ECs) and vascular smooth muscle cells (VSMCs) on native vascular extracellular matrix (ECM) scaffold in a rotary bioreactor. The expression levels of CD31, vWF, and the LDL uptake capacity, as well as the angiogenesis capability of the EC-like cells in the dynamic culture system were significantly enhanced compared to the static system. In addition, the α-actin and smoothelin expression, as well as contractility of VSMC-like cells harvested from the dynamic model were much higher than those in a static culture system. The combination of on-site differentiation of stem cells towards vascular cells in the natural vessel ECM scaffold and maturation of resulting vessel construct in a dynamic cell culture environment provides a promising approach to fabricating a clinically applicable vessel graft with similar mechanical properties and physiological functions of native blood vessels.

**Keywords**

Mesenchymal stem cell; differentiation; vascular tissue engineering; extracellular matrix scaffold; rotary bioreactor

## Introduction

Small-diameter vascular grafts are considered to be promising strategies to treat late stage vascular diseases, one of the largest causes of morbidity and mortality worldwide.[1-3] However, the current blood vessel substitutes are susceptible to failure mainly due to the mismatch in mechanical properties and biological functions with native vessels, and the rapid occlusion after implantation.[4, 5] Fabricating vascular conduits with replicated mechanical properties and biological functions of native blood vessels remains a great challenge.[6] Native blood vessels are composed of a single layer of endothelial cells (ECs) on the luminal surface and multiple layers of vascular smooth muscle cells (VSMCs) embedded in a fibrous extracellular matrix (ECM) of the blood vessel wall.[7] Functional VSMCs and ECs, as well as a vessel scaffold that can replicate the mechanical properties and biocompatibility of the native blood vessel wall are the three major elements of tissue-engineered blood vessels (TEBV). Compared to synthetic scaffolds which can provide desirable mechanical support to accommodate vascular cells and maintain durability *in vivo*,[8] native decellularized ECM provides not only excellent mechanical strength and biocompatibility, but also beneficial bioactive components for cell growth and stem cells differentiation in tissue engineering and regenerative medicine.[8-11]

Limited proliferation capacity and rapid cell function attenuation during *in vitro* expansion of primary vascular cells motivate the development of new approaches in which stem cells are induced to differentiate into ECs and VSMCs for vascular tissue engineering.[12-16] However, the differentiation of stem cells into vascular cells was usually promoted by chemical stimuli in planar culture system under static conditions,[17, 18] and the obtained cells have to be trypsinized and reseeded into the tubular scaffolds to constitute vessel grafts,[8, 14] which potentially impair the phenotype and function of resulting cells. In addition, VSMCs lying in the media of blood vessel

wall withstand tensile stress as the vessel dilates in response to the pulsatile pressure exerted by the cardiac cycle, while ECs lining the lumen of the vessels experience shear stress caused by blood flow.[19] These mechanical forces play a substantial role in the commitment of vascular cell functions and maintenance of vascular homeostasis.[19] However, the impact of these mechanical cues on stem cell differentiation towards ECs or VSMCs phenotype is not fully understood, despite the fact that some evidences suggested that the substrate stiffness was able to alter the differentiation of stem cells toward VSMCs and ECs.[20-23]

In this scenario, this study aims to compare the differentiation efficiency of human bone marrow derived mesenchymal stem cells (MSCs) towards ECs and VSMCs on a native vessel ECM scaffold in static culture system and in a dynamic cell culture system (rotary bioreactor). The mRNA and protein expression levels of the markers of ECs and VSMCs as well as ECs- and VSMCs-specific functions were compared for the two culture systems, where human aortic ECs and VSMCs were used as the positive controls, respectively. In this study, we hypothesize that the soluble growth factors directed differentiation of human MSCs towards VSMCs and ECs would be enhanced by the bioactive components of native arterial ECM and the mechanical stress generated in a rotary bioreactor.

## Materials and methods

### Preparation of decellularized ECM scaffolds and DNA quantification analysis.

The decellularized pig carotid artery scaffolds (Fig. 1A) were prepared according to the procedures described in our previous studies.[11] Briefly, carotid arteries were treated with 3-[(3-cholamidopropyl) dimethylammonio]-1-propanesulfonate (CHAPS) buffer (8 mM CHAPS, 1 M NaCl, and 25 mM EDTA) for 22 hours, followed by brief washes with PBS three times. Next,

carotid vessels were incubated with sodium dodexyl sulfate (SDS) buffer composed of 1.8 mM SDS, 1 M NaCl, and 25 mM EDTA for 24 hours, followed by complete washes with PBS ten times. Lastly, the carotid vessels were treated with 0.2 mg/ml DNase and 1 mg/ml RNase in PBS for 16 h at 37°C, and then washed thoroughly with PBS ten times. All reagents were bought from Sigma Aldrich (Sigma, St. Louis, MO).

The decellularization efficiency was determined by DNA quantification analysis as described in our previous study.[24] Briefly, the DNA content of fresh carotid arteries and decellularized vessel ECM scaffolds was measured using PicoGreen DNA assay following the protocol provided by the manufacturer (Invitrogen, Carlsbad, CA, USA). The fluorescence intensity for each sample was read at an excitation wavelength of 480 nm and an emission wavelength of 530 nm using a microplate reader (Infinite M200, Tecan, USA).

**On-site differentiation of MSCs on decellularized vascular ECM scaffold in a rotary bioreactor.**

Human bone marrow-derived MSCs ($P_1$-$P_5$) were cultured in MSC culture medium supplemented with MSC growth kit. Human aortic SMCs ($P_1$-$P_3$) were grown in vascular cell basal medium supplemented with VSMC growth kit. Human aortic ECs ($P_1$-$P_3$) were cultured in vascular cell basal medium supplemented with EC growth kit. The three types of cells were subcultured when they reached approximately 90% confluence and the medium was refreshed every other day. All cell lines, culture media, and growth kits were purchased from ATCC (Manassas, VA, USA)

To evaluate the combined effects of dynamic cell culture environment and the decellularized ECM scaffold on the differentiation of MSCs towards ECs, MSCs were grown

under different culture conditions as follows: (1) MSCs cultured in complete MSC medium were defined as MSC group; (2) MSCs seeded into the intimal surface of decellularized vessel ECM scaffolds ($1\times10^6$ cells/scaffold) and cultivated in complete EC medium supplemented with 50 ng/ml vascular endothelial growth factor (VEGF, Invitrogen, Carlsbad, CA, USA) were defined as Static group; (3) The cells harvested from the vessel ECM scaffold in an *ex vivo* blood vessel bioreactor system (Synthecon, Houston, TX) were defined as Dynamic group as schematically illustrated in Fig. 1.[25] A laminar perfusion system throughout the whole circuit driven by a digital peristaltic pump not only exerted longitudinal shear stress on the cells seeded on the luminal side of vessel scaffold, but also provided circumferential tensile stress for the cells grown on the adventitial side of vessel scaffold. The decellularized pig carotid artery scaffold was mounted onto the insert of the bioreactor under sterile conditions (Fig. 1B). A circuit was constructed after placing the insert back into the bioreactor (Fig. 1C). Thereafter, $1\times10^6$ MSCs in 2 ml EC medium supplemented in 50 ng/ml VEGF were injected into the lumen of vessel scaffold from the port at the end of rotary cylinder, and the rotary cylinder was rotated $90^o$ every 30 min for 4 h to promote cell attachment to the vessel ECM scaffold. Finally, the perfusion through the whole circuit was started at a low flow rate of 0.5 ml/min for the first 24 h, and then increased to 1.5 ml/min for the following two weeks; (4) ECs cultured in complete EC medium were used as a positive control.

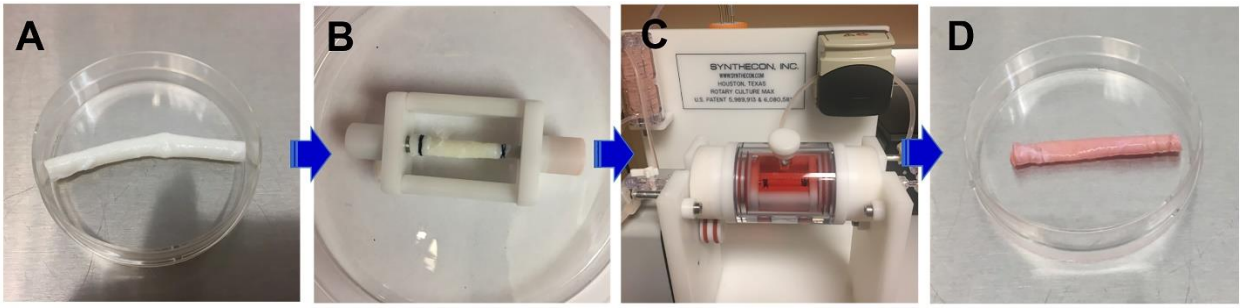


**Fig. 1** Schematic of the *ex vivo* bioreactor incorporated with a decellularized carotid artery scaffold. (A) Decellularized ECM scaffold. (B) MSCs were seeded on either intimal or adventitial side of decellularized carotid artery scaffold and mounted on the bioreactor insert. (C) The ECM-MSCs were cultured in vascular bioreactor with VEGF medium inside of the vessel scaffold and TGFβ1 medium outside of vessel scaffold. (D) The tissue engineered blood vessel (TEBV).

The differentiation of MSCs towards VSMCs in the bioreactor was conducted following a similar strategy that was used for the MSCs-ECs differentiation. (1) MSCs cultured in complete MSC medium were defined as MSC group; (2) MSCs seeded into the adventitial surface of decellularized vessel ECM scaffolds ($1\times10^6$ cells/scaffold) and maintained in complete MSCs medium supplemented with 10 ng/ml transforming growth factor-beta 1 (TGFβ1, Invitrogen, Carlsbad, CA, USA) were defined as Static group; (3) $1\times10^6$ MSCs were seeded manually onto the adventitial side of the vessel scaffold that was mounted on the insert of the bioreactor, and then the insert was placed back into the bioreactor and cultured overnight. Lastly, the perfusion was started at a lower flow rate of 0.5 ml/min for the first 24 h and followed by 1.5 ml/min for the rest of the two weeks of culture period. The cells harvested from the ECM scaffold cultured in the rotary bioreactor system were defined as the Dynamic group; (4) VSMCs cultured in complete VSMC medium were used as a positive control. All the cells were incubated at 37°C in a 5% $CO_2$ and 95% humidity environment, and fed every other day. After two-week incubation

in the rotary bioreactor, the engineered blood vessel was harvested for the vascular cell functional characterization (Fig. 1D).

**Mechanical force analysis for the bioreactor.**

The 2.5 cm long vessel scaffold (2.5 mm in diameter) in the bioreactor experiences forces derived from the pressure of the flowing media, the rotation of the scaffold, and the shear stress caused by the flowing media. The fluid velocity is calculated from the flow rate using Eq. 1:

$$v_f = Q/A \quad (1)$$

where $Q$ is the volumetric flow rate and $A$ is the cross-sectional area. The fluid pressure is given by Eq. 2:

$$P = \frac{1}{2}\rho v_f^2 \quad (2)$$

where $\rho$ is the density of the media, in this case assumed to be water at 1000 kg/m$^3$. Pressure within the vessel was calculated to be $1.25\times10^{-2}$ Pa. Multiplying by the surface area of the vessel yields a force of 2.45 μN. The rotational stress is given by Eq 3:

$$\sigma = \omega^2 \rho r^2 \quad (3)$$

where $\omega$ is the angular velocity, $\rho$ is the density of the tissue taken to be that of the muscle at 1059 kg/m$^3$,[26] and $r$ is the radius. Multiplying by the surface area gives the force over the whole scaffold at 3.39 μN. In the scaffold, the shear stress is given by Eq 4:

$$\tau = \mu \frac{v}{h} \quad (4)$$

where $\mu$ is the viscosity assumed to be that of water at $10^{-3}$ Pa•s, $v$ is the fluid velocity, and $h$ is the diameter of the scaffold. Multiplying the shear stress by the surface area of the scaffold yields a force of 0.39 μN.

**Cell viability evaluation, histological analysis, and scanning electron microscopy examination.**

***Cell viability evaluation***

To assess the effect of the dynamic culture system on MSCs viability, the cells grown on decellularized ECM for two weeks were stained with calcein-AM/EthD-1 solution (Invitrogen, Carlsbad, CA, USA) as reported previously.[24] Live cells were stained green because ubiquitous intracellular esterase activity is able to digest non-fluorescent calcein-AM into green fluorescent calcein, whereas dead cells were stained red since EthD-1 can pass through damaged membranes and emit red fluorescence upon binding to nucleic acids. The samples were observed under a confocal microscope (IX83 FV1200, Olympus Life Science, Center Valley, PA, USA).

***Histological analysis***

Fresh carotid arteries, decellularized vessel ECM scaffolds, and the cells-ECM constructs after a 14-day cultivation under mechanical stimulations in the rotary bioreactor, were fixed with 4% paraformaldehyde (Affymetrix, Santa Clara, CA, USA) at 4°C overnight, and washed three times with PBS. The paraffin-embedded sections (5 μm thickness) were prepared for staining with hematoxylin and eosin dyes (Sigma, St. Louis, MO, USA) or Masson's trichrome dyes (Sigma, St. Louis, MO, USA), respectively. Images were acquired with a phase contrast microscope (IX83, Olympus Life Science, Center Valley, PA, USA).

***Scanning electron microscopy observation***

After 14-day cultivation under mechanical stimulations in the bioreactor, the cells-ECM constructs were fixed with 2.5% glutaraldehyde (Sigma, St. Louis, MO, USA) overnight at 4°C, and dehydrated in a series of graded ethanol (25%, 50%, 75%, 95% and 100%) before lyophilization. The freeze-dried samples were then mounted onto stubs, sputtered with platinum, and observed with a scanning electron microscope (SEM, FEI Quanta 450, Beaverton, OR, USA).

**Gene expression by real-time RT-PCR analysis.**

To compare the mRNA expression levels of marker genes of ECs or VSMCs between different groups, total RNA was extracted using TRIzol reagent (Invitrogen, Carlsbad, CA, USA) according to the manufacturer's protocol, and quantified by spectrophotometric analysis at 260 nm. 200 ng RNA for each group was used for reverse transcription with a High Capacity cDNA Reverse Transcript kit (Applied Biosystems, Forster City, CA, USA). Lastly, real-time PCR was performed with Taqman gene expression assays (Applied Biosystems, Forster City, CA, USA) on a fast real-time PCR instrument (7500 Fast Real-Time PCR system, Applied Biosystems). The relative mRNA expression levels for CD31 (Hs01065279), von Willebrand factor (vWF, Hs01109446), fetal liver kinase-1 (flk-1, Hs00911700), α-actin (Hs00426835), calponin (Hs00206044), and smoothelin (Hs00199489) were estimated and normalized to β-actin (Hs01060665). Each sample was tested in triplicate.

**Evaluation of protein expression with immunofluorescence staining.**

The difference in ECs or VSMCs specific protein expression level between different groups was determined by immunostaining. The samples from each experimental group were fixed in 4% paraformaldehyde at 4°C overnight. The fixed vessel scaffolds seeded with cells in the static group and dynamic group were embedded in paraffin and sectioned to 5 μm thickness. After sequential treatment of antigen retrieval with 10 mM sodium citrate solution (Invitrogen, Carlsbad, CA, USA), permeabilizing with 0.5% Triton-X-100 solution (Sigma, St. Louis, MO, USA) and blocking with 1% bovine serum albumin (Sigma, St. Louis, MO, USA), the sections were stained with the following mouse anti-human antibodies (1:50): anti-CD31, anti-vWF, anti-flk-1, anti-smoothelin, anti-α-actin, and anti-calponin at 4°C overnight. After the complete rinses with PBS, the samples were incubated with the FITC-conjugated goat anti-mouse IgG (Invitrogen, Carlsbad, CA, USA) at 37°C for 2 h, and followed by staining with Hoechst 33342. The samples were observed under confocal microscopy. Except for the antibodies anti-α-actin and anti-calponin that were purchased from Sigma (St. Louis, MO, USA), all other antibodies used in this experiment were purchased from Abcam (Cambridge, MA, USA).

**EC-specific functional analysis.**

Acetylated low-density lipoprotein uptake assay was employed to perform the endothelial cells-specific functional analysis for the cells harvested from all four experimental groups. Briefly, the harvested cells from different groups were incubated with 10 μg/ml Dil-labeled acetylated low-density lipoprotein (Dil Ac-LDL, Invitrogen, Carlsbad, CA, USA) in serum-free medium at 37°C for 4 h, and followed by fixing with 4% paraformaldehyde. After that, the samples were stained with Hoechst 33342 to counterstain nuclei, and Dil Ac-LDL uptake was assessed quantitatively by confocal microscopy.

Angiogenesis assay was carried out using Matrigel solution (Corning) at 5 mg/ml. A 96-well plate was loaded with 50 μl Matrigel in each well, and then incubated at 37°C for 30 min before polymerization. The cells from different groups were harvested with trypsin and seeded on the Matrigel surface ($8\times10^3$ cells/well). After 24 h culture, five randomly selected fields for each sample were photographed with phase contrast microscope. The number of junctions and segments as well as total segments length within each image were analyzed using Image J.

**VSMC-specific functional analysis.**

Cell contractile capacity in different groups was evaluated by cell area reduction in response to vasoactive agonists as described in our previous study.[11] The cells from different groups were trypsinized and seeded in 24-well plate with a final concentration of $1\times10^4$ cells/well. After overnight-culture, the cells were stimulated with 50 mM KCl or 1 mM carbachol (Sigma, St. Louis, MO, USA) for 15 min. Images were acquired using a phase contrast microscope (IX83, Olympus Life Science, Center Valley, PA, USA), and the cell area reduction was analyzed with Image J.

Collagen gel contraction experiment was performed using rat tail collagen I solution (Corning, New York, USA) at 2 mg/ml. Briefly, the cells from different groups were trypsinized and mixed in a neutral collagen solution at $1.5\times10^5$ cells/ml cell density. Portions of 100 μl were added in 12-well plate (Corning, New York, USA) and allowed to gelate for 1.5 hour at 37°C. After that, the collagen gels were detached with a spatula and allowed to contract for 24 h or 48 h. Images were captured using a stereo microscope (SZX10, Olympus Life Science, Center Valley, PA, USA) with a digital camera (DP22, Olympus Life Science, Center Valley, PA, USA), and the areas of contracted gels were calculated using Image J.

**Statistical analysis.**

All data were expressed as mean ± standard error of mean (SEM). Statistical analysis was performed by two-sample *t* test assuming equal variances, and $P < 0.05$ was considered statistically significant.

## Results

### Characterization of decellularized vessel scaffolds

To determine the decellularization efficiency, Hematoxylin and Eosin (H&E) staining of both native carotid and decellularized ECM scaffolds were performed and the results (Fig. S1) clearly showed that cellular and nucleic components were completely removed in the decellularized ECM (Fig. S1C, 1D) compared to native carotid (Fig. S1A, 1B). Furthermore, decellularized ECM scaffolds showed an average residual DNA of 0.018 ± 0.005 μg/mg, which was significantly lower than 0.213 ± 0.026 μg/mg contained in the native carotid (Fig. S1E). The significantly decreased remaining DNA content in the decellularized scaffolds supported the histological staining observations.

### Cell viability and morphology of EC-like cells grown on the luminal side of decellularized ECM scaffold in bioreactor

Cell viability and morphological characteristics of the EC-like cells grown on the luminal side were examined to evaluate the effect of the dynamic microenvironment provided by both the ECM and bioreactor on MSCs differentiation. The cell viability was evaluated by live-dead staining after two-week culture in the dynamic model. As shown in the Fig. 2A, MSCs reseeded

on the intimal side of decellularized ECM scaffold in the dynamic cell culture system displayed high cell viability after two weeks, indicating that a beneficial microenvironment was provided by the dynamic cell culture model. In addition, the intimal surface of ECM scaffolds recellularized with MSCs was observed by SEM. After two weeks of cultivation, an intact cell layer covered with secreted matrix was observed on the intimal surface of decellularized scaffold (Fig. 2B). Moreover, both HE staining and Masson's trichrome staining were applied to visualize the morphological characteristics of MSCs loaded into the dynamic cell culture system. A dense EC-like cells layer was formed on the intimal side of decellularized ECM scaffold (Fig. 2C-2F). All these observations supported the fact that the combination of decellularized ECM and the mechanical force generated by the rotary bioreactor was favorable for MSCs attachment, growth, and differentiation.

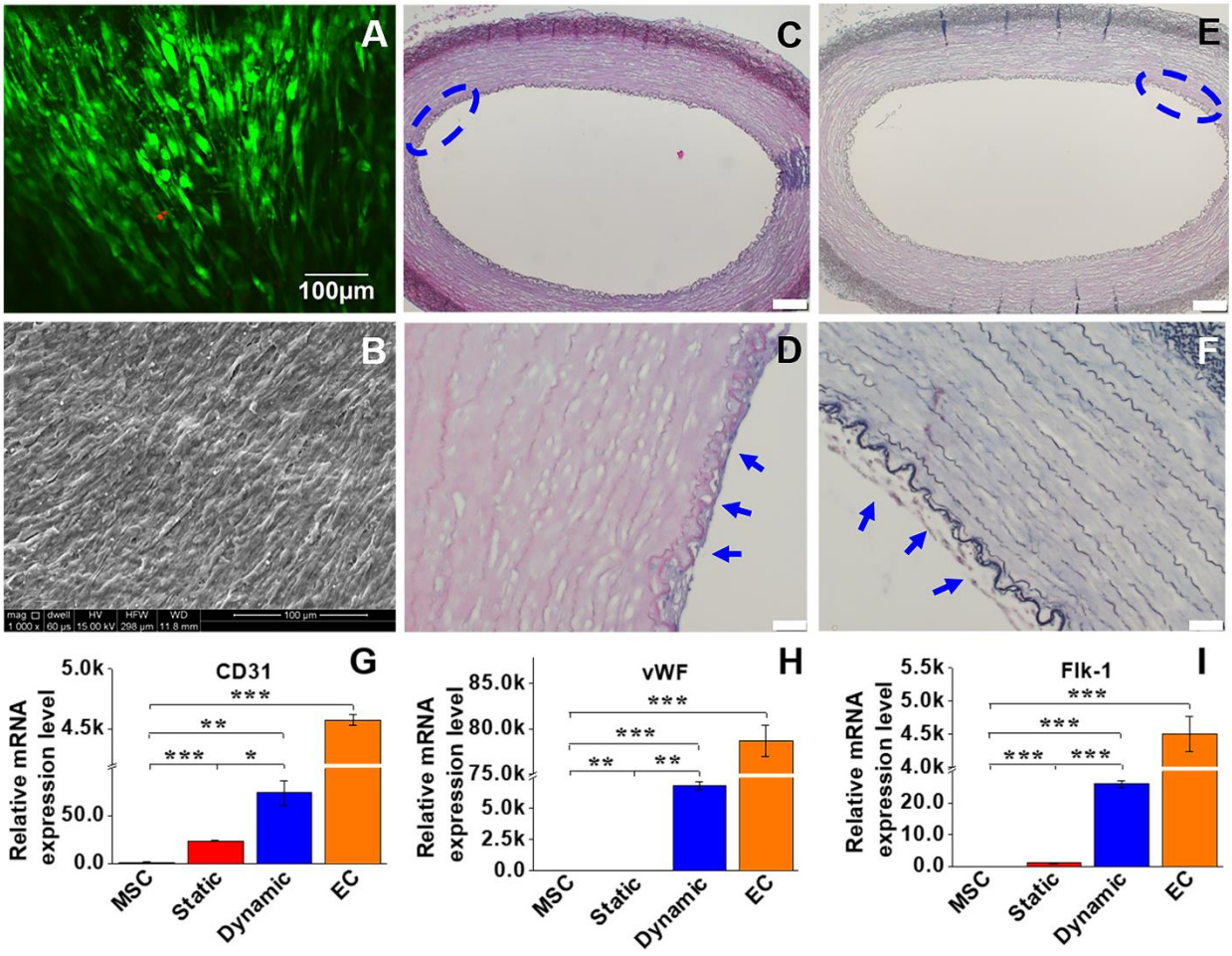


**Fig. 2** Cell viability and morphological characteristics, and real time RT-PCR analysis for the ECs marker genes expressions. (A) MSCs reseeded on the intimal side of decellularized ECM in the dynamic model displayed high cell viability after two weeks. (B) An intact cell layer covered with secreted ECM was observed on the intimal surface of decellularized scaffolds. (C, D) H&E staining and (E, F) Masson's trichrome staining confirmed that a dense layer of EC-like cells was formed on the intimal side of decellularized ECM (blue arrows). Each marker gene was significantly upregulated for both static and dynamic groups compared to negative control (MSCs), and the transcript expression level of each marker gene in dynamic culture system was significantly higher than that in static culture system. Data are expressed as mean ± SEM ($n$=3). *$P$ < 0.05, **$P$ < 0.01, ***$P$ < 0.001.

**Gene and protein expression of EC-specific markers.**

To compare the differentiation efficiency of MSCs towards EC-like cells in the static culture system and in the dynamic bioreactor system, both the mRNA expression and protein expression levels of three EC-specific markers were determined by real time RT-PCR and immunofluorescence staining, respectively. As shown in Fig. 2G-2I, each marker gene, including CD31, vWF, and flk-1 was significantly upregulated in both the static and dynamic group compared to MSCs (negative control), but lower than ECs (positive control). More importantly, the transcript expression level of each marker gene in the dynamic culture system was significantly higher than that of the static culture system, suggesting the substantial roles played by mechanical forces in facilitating the VEGF-directed differentiation of MSCs towards EC-like phonotype. Consistent with the real-time PCR results, immunofluorescence staining for CD31 and vWF showed the protein expression levels in the dynamic group were much higher than those in the static group and MSCs control (Fig. 3), although they were still lower than those in ECs (positive control). These results provide robust evidence for the fact that the dynamic culture system incorporated with native vascular ECM exerted an important regulatory role in MSCs-ECs differentiation.

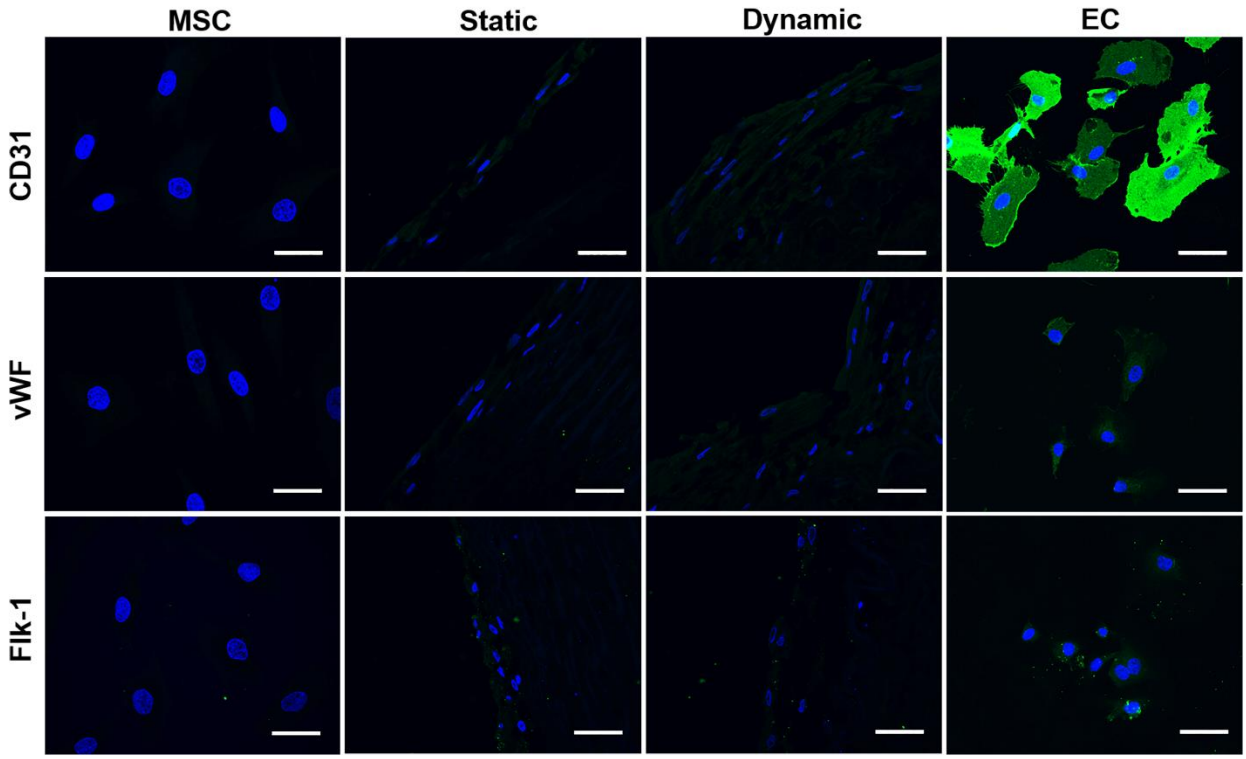


**Fig. 3** Immunofluorescent staining for EC-specific proteins CD31, vWF, and flk-1. Each marker protein expression level in both the static and dynamic groups was much higher than that in the MSCs control group. Both CD31 and vWF expression levels in the dynamic group were stronger than those in the static group. The images represent at least three independent experiments. Scale bars = 50 μm.

**Functional evaluation of the MSCs-derived EC-like cells.**

LDL uptake assay and Matrigel angiogenesis were employed to detect the functional activity of EC-like cells differentiated from MSCs in the different culture systems. As shown in Fig. 4A-4D, MSCs (negative control) were unable to uptake Dil Ac-LDL, whereas positive control ECs exhibited high Dil Ac-LDL uptake capacity. Compared to the cells in the static group with a low capability to uptake Dil Ac-LDL, the cells differentiated from the dynamic group showed much higher Dil Ac-LDL uptake capacity, indicating the high MSCs-ECs differentiation efficiency under shear stress stimulation. The capabilities of four different cell groups to form capillary

networks was tested on Matrigel (Fig. 4E-4H). The negative control MSCs exhibited a low capacity to form capillary networks (Fig. 4E), whereas a dense capillary network was generated by control ECs on Matrigel after 24 h (Fig. 4H). The cells differentiated in the static group (Fig. 4F) evidently formed more networks than the MSCs group, but much less than the dynamic group (Fig. 4G). Quantitative analysis on junction number, segments number, and total segments length for each group was further performed to compare their network formation capabilities. All quantitative parameters of the dynamic group were significantly higher than those of the static group (Fig. 4I-4K). Taken together, consistent with genetic and protein assays, all the functional evaluation results supported that the microenvironment provided by the native carotid ECM and mechanical cues generated in the bioreactor was able to enhance the MSCs-ECs differentiation.

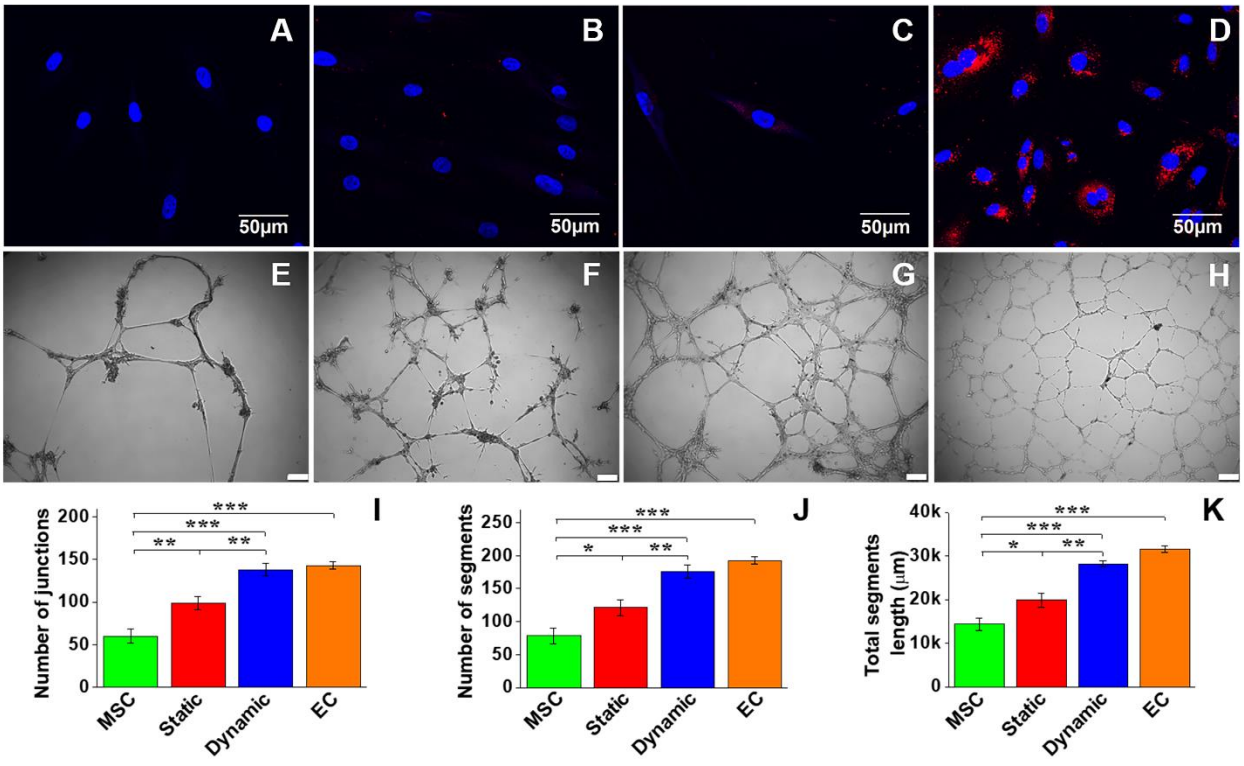


**Fig. 4** LDL-uptake assay and Matrigel angiogenesis evaluation of MSC-derived EC-like cells. Negative control MSCs were unable to uptake Dil Ac-LDL (A), whereas positive control ECs exhibited a high capability of uptaking Dil Ac-LDL (D). Compared to the static culture group

(B), the dynamic culture group showed a much higher Dil Ac-LDL uptake capability (C). Negative control MSCs showed a small amount of capillary network formed on Matrigel after 24 h (E). In contrast, a dense capillary network was generated by positive control ECs on Matrigel after 24 h (H). The cells for the static group (F) apparently formed more networks than the MSCs group, but much less than the dynamic group (G). Scale bars = 100 μm. Quantitative analysis on the parameters of capillary network showed the significant differences existed among the four different cell groups (I-K). Data are expressed as mean ± SEM of five randomly selected images (48 cm×36 cm). *$P < 0.05$, **$P < 0.01$, ***$P < 0.001$.

**Cells viability and morphology of VSMC-like cells differentiated on the adventitial side of ECM scaffold in bioreactor**

To evaluate the effect of the microenvironment provided by the adventitial side of the ECM scaffold on cell viability, live-dead staining was also conducted for the dynamic model after two weeks of culture. As shown in Fig. 5A, MSCs seeded on the outside surface of the ECM scaffold exhibited high viability on day 14, supporting the fact that the dynamic culture system with a decellularized ECM is favorable for MSCs survival on both the intimal and adventitial sides. SEM imaging further demonstrated that MSCs seeded on the adventitial side of ECM scaffold were able to secrete ECM proteins and form an intact cell layer with a uniform topology after two weeks of cultivation (Fig. 5B). The histological morphology of the dynamic cell group was characterized by both H&E and Masson's trichrome staining (Fig. 5C-5F), where a number of VSMC-like cell layers were formed on the adventitial surface of vessel scaffolds. Therefore, the decellularized carotid ECM is an ideal scaffold to support MSCs growth and differentiation on both sides for fabricating vessel grafts for vascular tissue engineering.

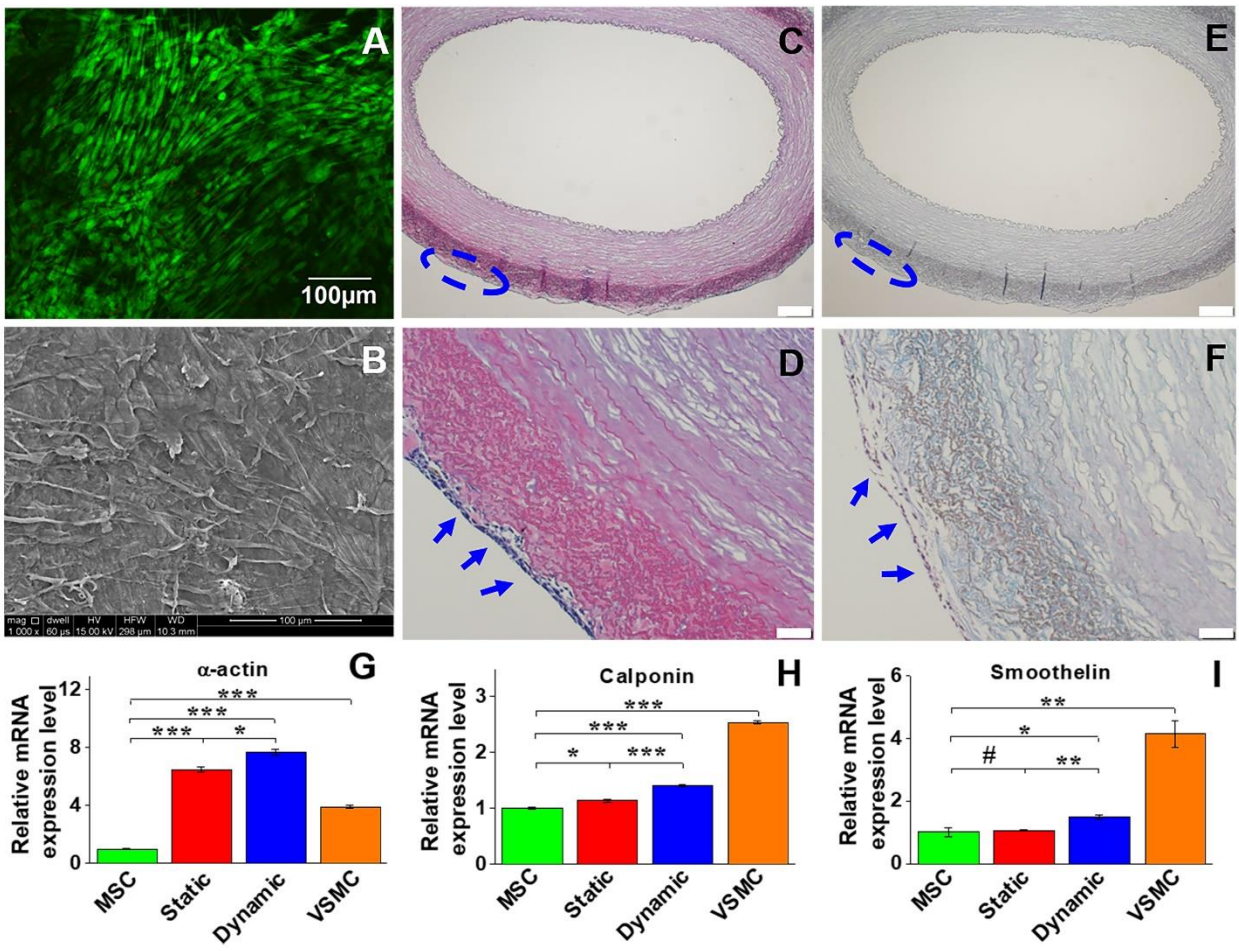


**Fig. 5** Cell viability and morphology, and mRNA expression of VSMC marker proteins in different experimental groups. Live-dead staining showed cells cultured on the adventitial side of vessel scaffold exhibited high viability on day 14 (A). SEM imaging also demonstrated that the cells cultured in the dynamic system were able to form an intact cell layer with uniform topology after two weeks (B). H&E staining (C, D) and Masson's trichrome staining (E, F) showed multiple layers of VSMC-like cells grown on the adventitial side of vessel scaffolds (blue arrows). Real time RT-PCR revealed that gene expression of α-actin and calponin was significantly upregulated in each differentiation group compared to the control MSCs (G). The mRNA expression level of each marker protein in the dynamic group was significantly higher than that in the static group, and α-actin expression levels in both the dynamic and static groups were even higher than that in positive control VSMCs (G). Data are expressed as mean ± SEM ($n$=3). # $P > 0.05$, *$P < 0.05$, **$P < 0.01$, ***$P < 0.001$.

**Evaluation of mRNA and protein expression of VSMC markers.**

The expression levels of the three VSMC marker proteins, α-actin, calponin, and smoothelin were quantitatively analyzed at both transcript and protein expression levels by real time RT-PCR and immunostaining. As shown in Fig. 5G-5I, α-actin and calponin were significantly upregulated in each experimental group compared to the negative control (MSCs). The mRNA expression levels of all three VSMC marker proteins in the dynamic culture group were statistically higher than those in the static group, and α-actin expression levels in both dynamic and static groups were even higher than that of the positive control group (VSMCs). Consistent with the real time RT-PCR results, immunostaining for different cell groups also demonstrated that the fluorescence intensity of α-actin in the dynamic group was higher than that in the static group, and smoothelin was slightly upregulated in the dynamic group compared to the static group (Fig. 6). These results indicated that the combination of a decellularized vessel ECM and the circumferential tensile stress generated in a rotary bioreactor benefited the TGFβ1-induced MSCs-VSMCs differentiation.

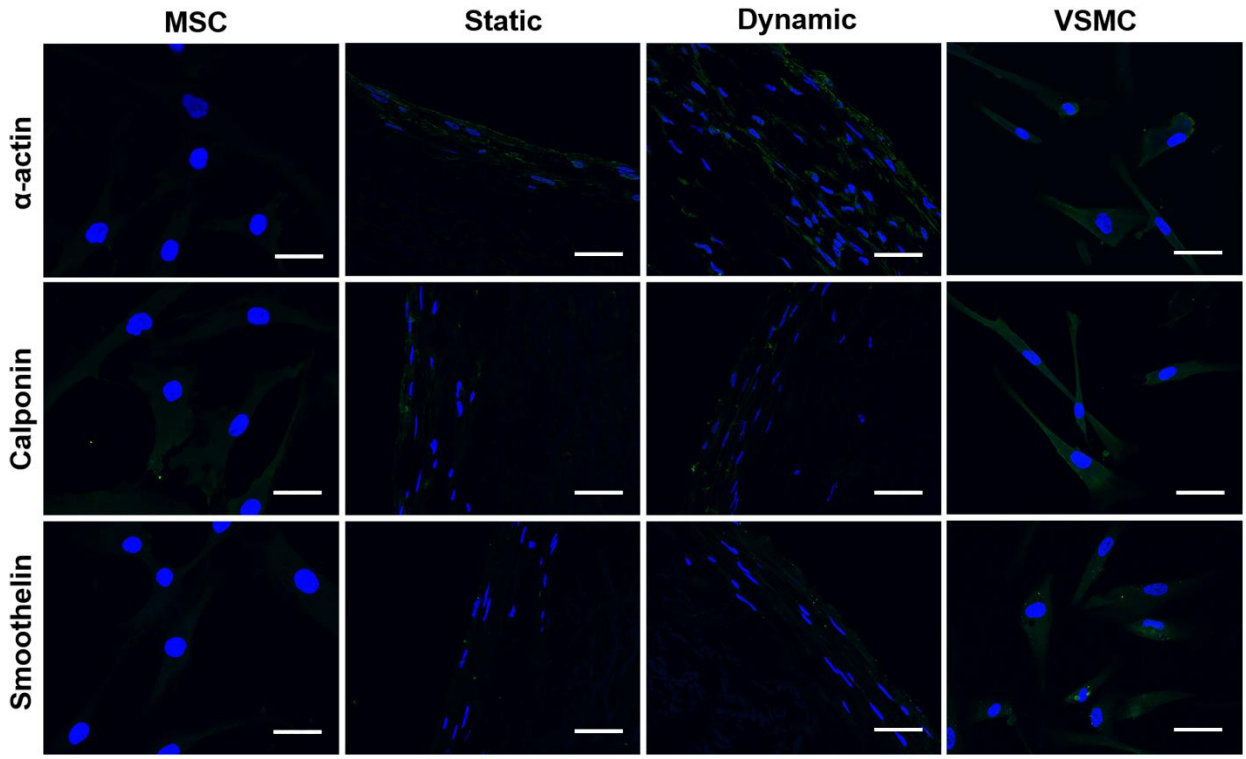


**Fig. 6** Immunostaining of VSMC marker proteins for different cell groups. The fluorescence intensity of α-actin in the dynamic group was much higher than that in the static group, and smoothelin in the dynamic group was slightly upregulated compared to the static group. The images represent at least three independent experiments. Scale bars = 50 μm.

**Functional analysis of the MSCs-derived VSMC-like cells.**

To further test the roles played by the dynamic culture system in MSCs-VSMCs differentiation, cell area reduction upon treatment with vasoactive agonists and collagen gel contraction capability were evaluated for the different cell groups. As shown in Fig. S2 and Fig. S3, most of the cells in each group appeared to contract in response to both KCl and carbachol. Negative control MSCs exhibited the lowest contractile capability with 16.54 ± 2.21% and 13.58 ± 1.42% cell area reduction upon exposure to KCl (Fig. 7A) and carbachol (Fig. 7B), respectively. Both KCl and carbachol induced significantly more reduction in cell area for static and dynamic groups compared to MSCs, and the reduction percentage of the cell area for dynamic group was

higher than that of static group.

Collagen lattice contraction assay was conducted to further evaluate cell contractility. As shown in Figure 7C, all four cell groups embedded in collagen gel could induce apparent contraction of the gel as culture time increased, and positive VSMCs group displayed the highest contractile capability. Quantitative analysis demonstrated that both the static and dynamic groups had a significantly higher level of contraction of collagen lattices compared to the MSCs group, and the dynamic group exhibited a slightly higher capacity of gel contraction compared to the static group ($p$>0.05) (Fig. 7D-7E), which is consistent with the results of real time RT-PCR and immunostaining assay.

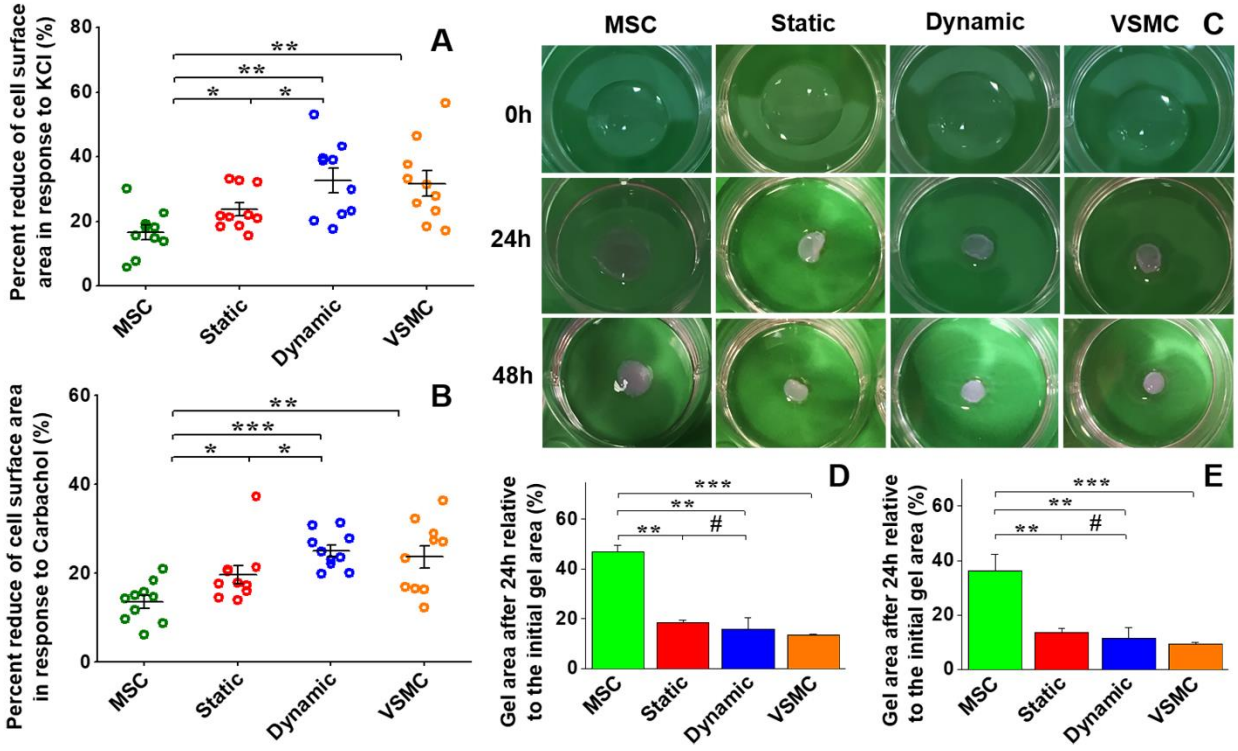


**Fig. 7** Functional analysis of MSC-derived VSMC-like cells. Cell area reduction assay showed that MSCs has the lowest contractile capability upon exposure to KCl (A) and carbachol (B), respectively. Both KCl and carbachol induced significant decreases in cell area for static and dynamic groups compared to the negative control MSCs, and the cell area for the dynamic group reduced more than that for the static group (A, B). Collagen lattice contraction assay showed

four groups of cells embedded in collagen gel could induce apparent contraction of the collagen gel, and positive VSMCs group exhibited the highest contraction capability among others (C). Quantitative analysis demonstrated that there was no significant difference between the collagen gel areas for the static and dynamic groups (D, E). Data are expressed as mean ± SEM ($n$=3). # $P > 0.05$, *$P < 0.05$, **$P < 0.01$, ***$P < 0.001$.

## Discussion

In this study, we developed a potential approach to fabricating an autologous vessel graft for vascular tissue engineering by the combination of an on-site differentiation of human bone marrow derived MSCs towards vascular cells on the natural blood vessel ECM scaffold and maturation of the vessel construct in a dynamic cell culture system. The powerful combinatorial promotive effect of the native vascular ECM scaffold and the mechanical cues generated by a rotary bioreactor on the MSCs differentiation was evaluated by comparing the differentiation efficiency and the physiological functions of resulting cells with that of the static cell culture system. Growth factors VEGF and TGFβ1 were respectively used as chemical cues to induce the differentiation of MSCs towards ECs and VSMCs in both dynamic and static culture systems.[27-30] Our results demonstrated that the cells cultured on the native vessel ECM scaffold in the dynamic system significantly increased the efficiency of the MSCs differentiation towards both EC and VSMC-like cells compared to the static culture system as evidenced by the upregulated expression of marker proteins for ECs (Fig. 2 and Fig. 3) and VSMCs (Fig. 5 and Fig. 6), as well as elevated EC- (Fig. 4) and VSMC- (Fig. 7) specific physiological functions.

The endothelial layer provides multiple anti-thrombogenic functions for native blood vessels, thus a lack of ECs lining the autologous vessel graft lumen is considered one of the major problems that may potentially cause a poor patency of engineered vessel constructs.[6, 31-33] In this study, the EC-like cells obtained by the on-site differentiation of MSCs on a

decellularized vessel scaffold could potentially overcome this drawback caused by the ECs deficiency in the engineered vessel graft. EC-like cells differentiated from MSCs in a static culture system incorporated with decellularized carotid scaffold exhibited a much higher EC-specific functions compared to negative control MSCs (Fig. 4). It is consistent with a recent report that decellularized ovine arteries matrix could serve as an efficient culture system for promoting differentiation of adipose-derived MSCs toward ECs.[34] The capability of the decellularized carotid vessel scaffold to facilitate MSCs-VSMCs differentiation has been reported in our previous study.[11] In addition, decellularized ECM was also reported to direct MSCs differentiation towards other directions that facilitate tissue regeneration, such as osteogenic and chondrogenic differentiation.[35, 36] The underlying mechanism by which the decellularized ECM scaffold promotes MSC-vascular cells differentiation may lie in the bioactive component proteins in the ECM, such as laminin, fibronectin, vitronectin, collagen, and gelatin.[37-39] For example, laminin played a critical role in enhancing the expression of EndoTF FOXC2 and its downstream gene, thereby inducing the endothelial differentiation of MSCs.[37] Gluck et al. found that laminin and vitronectin enhanced vascular ECs differentiation in a traditional 2D cell culture system, while fibronectin enhanced VSMCs differentiation in a 3D system.[38] More importantly, optimal combinatorial ECMs were able to enhance endothelial differentiation, compared to many single-factor ECMs, in part through an integrin β3-mediated pathway.[39] Furthermore, an ideal mechanical support provided by each side of native vascular ECM might be another reasonable explanation for the inductive effect on the MSCs differentiation exerted by ECM. A similar finding was reported by Wingate et al. that lineage commitment of MSCs towards specific vascular cells could be controlled by carefully designing the substrate modulus.[40] Additionally, MSCs cultured on poly(ε-caprolactone) (PCL) films with

uniaxial stretching have been demonstrated to obtain a contractile SMCs-like phenotype, with ordered organization of cellular stress filaments and upregulated expression of the contractile makers, including SM-α-actin, calponin, and SM-MHC.[41] Floren et al. also reported on the ability to augment MSCs differentiation into mature VSMCs by combining appropriate silk fibroin hydrogel stiffness (33 kPa) with growth factor (TGFβ1).[20]

In addition to the native vascular ECM, mechanical cues generated by a rotary bioreactor is a critical contributor to the dynamic cell culture system developed in this study for the differentiation of MSCs toward vascular cells and integrated with the ECM scaffold to form a physiologically functional vascular graft. Actually, it is well recognized that perfusion bioreactor systems are beneficial for vascular tissue engineering because they expose the vascular cells to flow and shear stress, which affect various cellular responses, arterial formation, and maintenance.[42] Therefore, chemical factor treatments may not be sufficient to develop tissue engineered vascular grafts and co-administration of biomechanical forces may be needed to improve stem cell differentiation.[43] Our findings are consistent with previous studies performed by Hasanzadeh et al. that shear stress exerted by blood flow alone could be an effective promoter for the differentiation of adipose-derived MSCs towards ECs.[44] Growing evidence supports the hypothesis that biomechanical cues play important roles in vascular cells derivation from stem cells.[43, 45, 46] Sivarapatna et al. reported that a biomimetic flow bioreactor was an effective means for the human induced pluripotent stem cells-ECs differentiation toward an arterial-like phenotype,[43] and shear force was also documented to exert a synergistic effect with VEGF in promoting the differentiation of adipose-derived stem cells into ECs.[45, 46] Additionally, similar to our studies, Park et al. compared the effects of biaxial and uniaxial strain on the differentiation of bone marrow MSCs, and reported that uniaxial strain, a better mimicked mechanical

environment experienced by VSMCs *in vivo*, could successfully promote MSCs differentiation towards VSMCs.[47] More specifically, mechanical stress causes VSMCs to have proper cellular orientation, increased synthesis of collagen fiber bundles, and altered phenotype from synthetic to contractile.[42] The study by Lee et al. was able to support that cell spreading, stress fiber formation, and apparent microvascular formation by ECs and MSCs in collagen gels are affected by fluid shear stress.[48] In terms of the underlying mechanism relating to how mechanical cues regulate the differentiation of MSCs into vascular cells, Kurpinski et al. interpreted that cells adjust their orientation along the direction of mechanical forces to minimize the stress applied on the cytoskeleton and other cellular components, and this adaptation in cell orientation may in turn influence MSC differentiation.[47, 49, 50] Besides, growing evidence supports that genes responsive to shear stress are connected to cell proliferation and differentiation, vascular tone, cellular adhesion, and immune responses.[42]

## Conclusions

Our findings demonstrate that the growth factors VEGF and TGFβ1 directed differentiation of human MSCs towards VSMCs and ECs can be significantly enhanced by the synergistic combination of bioactive components of native arterial ECM and mechanical forces in a dynamic cell culture system. These on-site differentiated vascular cells are able to integrate into a native vascular ECM scaffold and the vessel construct can be further matured under mechanical stimulation in a rotary bioreactor, thus providing a potential approach to fabricating a clinically available vessel graft with similar mechanical properties and biological functions of native blood vessels. Future work of this study will be to implant the engineered vessel graft into a model host to study its application in vascular tissue engineering.

## Funding

This work was supported in part by the American Heart Association (15SDG25420001), South Dakota Board of Regents (UP1600205) and National Science Foundation/EPSCoR Cooperative Agreement (IIA-1355423).

## Data Availability

All experimental data required to reproduce the findings from this study will be made available upon request.

## References

1. B. Unal, J. A. Critchley and S. Capewell, *Journal of Epidemiology and Community Health*, 2003, **57**, 530-535.
2. L. J. Laslett, P. Alagona, B. A. Clark, J. P. Drozda, F. Saldivar, S. R. Wilson, C. Poe and M. Hart, *Journal of the American College of Cardiology*, 2012, **60**, S1-S49.
3. B. C. Isenberg, C. Williams and R. T. Tranquillo, *Circulation Research*, 2006, **98**, 25-35.
4. H. H. Greco Song, R. T. Rumma, C. K. Ozaki, E. R. Edelman and C. S. Chen, *Cell Stem Cell*, 2018, **22**, 608.
5. H. Kurobe, M. W. Maxfield, C. K. Breuer and T. Shinoka, *Stem Cells Translational Medicine*, 2012, **1**, 566-571.
6. M. Meiring, M. Khemisi, L. Laker, P. M. Dohmen and F. E. Smit, *Medical Science Monitor Basic Research*, 2017, **23**, 344-351.
7. L. Zhang, J. Y. Zhou, Q. P. Lu, Y. J. Wei and S. S. Hu, *Biotechnology and Bioengineering*, 2008, **99**, 1007-1015.
8. Y. L. Zhao, S. Zhang, J. Y. Zhou, J. L. Wang, M. C. Zhen, Y. Liu, J. B. Chen and Z. Q. Qi, *Biomaterials*, 2010, **31**, 296-307.
9. J. Negishi, Y. Hashimoto, A. Yamashita, Y. W. Zhang, T. Kimura, A. Kishida and S. Funamoto, *Journal of Biomedical Materials Research Part A*, 2017, **105**, 1293-1298.
10. N. Syazwani, A. Azhim, Y. Morimoto, K. S. Furukawa and T. Ushida, *Journal of Medical and Biological Engineering*, 2015, **35**, 258-269.
11. N. Li, H. Sanyour, T. Remund, P. Kelly and Z. K. Hong, *Materials Science & Engineering C-Materials for Biological Applications*, 2018, **93**, 61-69.
12. S. W. Cho, H. J. Park, J. H. Ryu, S. H. Kim, Y. H. Kim, C. Y. Choi, M. J. Lee, J. S. Kim, I. S. Jang, D. I. Kim and B. S. Kim, *Biomaterials*, 2005, **26**, 1915-1924.
13. Y. S. Song, H. J. Lee, I. H. Park, W. K. Kim, J. H. Ku and S. U. Kim, *International Journal of Impotence Research*, 2007, **19**, 378-385.
14. B. C. Dash, K. Levi, J. Schwan, J. Luo, O. Bartulos, H. W. Wu, C. H. Qiu, T. Yi, Y. M. Ren, S. Campbell, M. W. Rolle and Y. B. Qyang, *Stem Cell Reports*, 2016, **7**, 11-20.

15. S. Sundaram, A. Echter, A. Sivarapatna, C. H. Qiu and L. Niklason, *Tissue Engineering Part A*, 2014, **20**, 740-750.
16. Y. Y. Wang, J. Hu, J. Jiao, Z. N. Liu, Z. Zhou, C. Zhao, L. J. Chang, Y. E. Chen, P. X. Ma and B. Yang, *Biomaterials*, 2014, **35**, 8960-8969.
17. C. G. Wang, Y. Li, M. Yang, Y. H. Zou, H. H. Liu, Z. Y. Liang, Y. Yin, G. C. Niu, Z. G. Yan and B. H. Zhang, *European Journal of Vascular and Endovascular Surgery*, 2018, **55**, 257-265.
18. C. Wang, S. Yin, L. Cen, Q. H. Liu, W. Liu, Y. L. Cao and L. Cui, *Tissue Engineering Part A*, 2010, **16**, 1201-1213.
19. K. Henderson, A. D. Sligar, V. P. Le, J. Lee and A. B. Baker, *Advanced Healthcare Materials*, 2017, **6**.
20. M. Floren, W. Bonani, A. Dharmarajan, A. Motta, C. Migliaresi and W. Tan, *Acta Biomaterialia*, 2016, **31**, 156-166.
21. A. M. Handorf, Y. X. Zhou, M. A. Halanski and W. J. Li, *Organogenesis*, 2015, **11**, 1-15.
22. R. Subbiah, M. P. Hwang, P. Du, M. Suhaeri, J. H. Hwang, J. H. Hong and K. Park, *Macromolecular Bioscience*, 2016, **16**, 1723-1734.
23. K. Wingate, M. Floren, Y. Tan, P. O. N. Tseng and W. Tan, *Tissue Engineering Part A*, 2014, **20**, 2503-2512.
24. N. Li, D. D. Wang, Z. G. Sui, X. Y. Qi, L. Y. Ji, X. L. Wang and L. Yang, *Tissue Engineering Part C-Methods*, 2013, **19**, 708-719.
25. Q. Shi, V. Hodara, C. R. Simerly, G. P. Schatten and J. L. VandeBerg, *Stem Cells and Development*, 2013, **22**, 631-642.
26. S. R. Ward and R. L. Lieber, *Journal of Biomechanics*, 2005, **38**, 2317-2320.
27. M. Seruya, A. Shah, D. Pedrotty, T. du Laney, R. Melgiri, J. A. McKee, H. E. Young and L. E. Niklason, *Cell Transplantation*, 2004, **13**, 93-101.
28. B. Kinner, J. M. Zaleskas and M. Spector, *Experimental Cell Research*, 2002, **278**, 72-83.
29. M. Y. Chen, P. C. Lie, Z. L. Li and X. Wei, *Experimental Hematology*, 2009, **37**, 629-640.
30. M. B. Nourse, D. E. Halpin, M. Scatena, D. J. Mortisen, N. L. Tulloch, K. D. Hauch, B. Torok-Storb, B. D. Ratner, L. Pabon and C. E. Murry, *Arteriosclerosis Thrombosis and Vascular Biology*, 2010, **30**, 80-U189.
31. S. L. Mitchell and L. E. Niklason, *Cardiovascular Pathology*, 2003, **12**, 59-64.
32. V. Barron, E. Lyons, C. Stenson-Cox, P. E. McHugh and A. Pandit, *Annals of Biomedical Engineering*, 2003, **31**, 1017-1030.
33. J. M. M. Heyligers, C. H. P. Arts, H. J. M. Verhagen, P. G. de Groot and F. L. Moll, *Annals of Vascular Surgery*, 2005, **19**, 448-456.
34. W. B. Zhang, Y. H. Huo, X. L. Wang, Y. M. Jia, L. Su, C. X. Wang, Y. Li, Y. H. Yang and Y. Y. Liu, *Heart and Vessels*, 2016, **31**, 1874-1881.
35. C. Y. Gao, Z. H. Huang, W. Jing, P. F. Wei, L. Jin, X. H. Zhang, Q. Cai, X. L. Deng and X. P. Yang, *Journal of Materials Chemistry B*, 2018, **6**, 7471-7485.
36. Y. Liang, E. Idrees, A. R. A. Szojka, S. H. J. Andrews, M. Kunze, A. Mulet-Sierra, N. M. Jomha and A. B. Adesida, *Acta Biomaterialia*, 2018, **80**, 131-143.
37. C. H. Wang, T. M. Wang, T. H. Young, Y. K. Lai and M. L. Yen, *Biomaterials*, 2013, **34**, 4223-4234.
38. J. M. Gluck, C. Delman, J. Chyu, W. R. MacLellan, R. J. Shemin and S. Heydarkhan-Hagvall, *Journal of Biomedical Materials Research Part B-Applied Biomaterials*, 2014, **102**, 1730-1739.
39. L. Q. Hou, J. J. Kim, M. Wanjare, B. Patlolla, J. Coller, V. Natu, T. J. Hastie and N. F. Huang, *Scientific Reports*, 2017, **7**.
40. K. Wingate, W. Bonani, Y. Tan, S. J. Bryant and W. Tan, *Acta Biomaterialia*, 2012, **8**, 1440-1449.
41. Z. Y. Wang, S. H. Teoh, N. B. Johana, M. S. K. Chong, E. Y. Teo, M. H. Hong, J. K. Y. Chan and E. S. Thian, *Journal of Materials Chemistry B*, 2014, **2**, 5898-5909.
42. M. B. Elliott and S. Gerecht, *Journal of Materials Chemistry B*, 2016, **4**, 3443-3453.

43. A. Sivarapatna, M. Ghaedi, A. V. Le, J. J. Mendez, Y. B. Qyang and L. E. Niklason, *Biomaterials*, 2015, **53**, 621-633.
44. E. Hasanzadeh, G. Amoabediny, N. Haghighipour, N. Gholami, J. Mohammadnejad, S. Shojaei and N. Salehi-Nik, *In Vitro Cellular & Developmental Biology-Animal*, 2017, **53**, 818-826.
45. L. J. Fischer, S. McIlhenny, T. Tulenko, T. Tulenko, N. Golesorkhi, P. Zhang, R. Larson, J. Lombardi, I. Shapiro and P. J. DiMuzio, *Journal of Surgical Research*, 2009, **152**, 157-166.
46. F. Colazzo, F. Alrashed, P. Saratchandra, I. Carubelli, A. H. Chester, M. H. Yacoub, P. M. Taylor and P. Somers, *Growth Factors*, 2014, **32**, 139-149.
47. J. S. Park, J. S. F. Chu, C. Cheng, F. Q. Chen, D. Chen and S. Li, *Biotechnology and Bioengineering*, 2004, **88**, 359-368.
48. E. J. Lee and L. E. Niklason, *Tissue Engineering Part C-Methods*, 2010, **16**, 1191-1200.
49. K. Kurpinski, J. Chu, C. Hashi and S. Li, *Proceedings of the National Academy of Sciences of the United States of America*, 2006, **103**, 16095-16100.
50. K. Kurpinski, J. Chu, D. J. Wang and S. Li, *Cellular and Molecular Bioengineering*, 2009, **2**, 606-614.

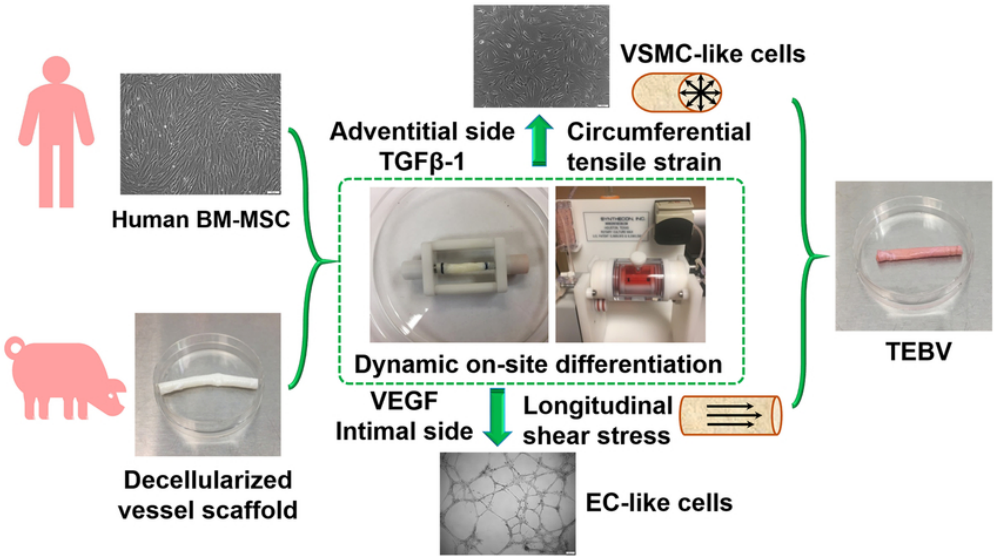


72x40mm (300 x 300 DPI)

Stem cell differentiation on the decellularized native blood vessel scaffold under mechanical stimulation for vascular tissue engineering